A 2D processing algorithm for detecting landmines using Ground Penetrating Radar data.

Mr. Anand Sengodan and Dr. W. Paul Cockshott
Computer Vision and Graphics Group
School of Computing Science
University of Glasgow
Glasgow, G12 8QQ
Email: {sengodan, wpc}@dcs.gla.ac.uk

***Abstract*— Ground Penetrating Radar(GPR) is one of a number of technologies that have been used to improve landmine detection efficiency. The clutter environment within the first few cm of the soil where landmines are buried, exhibits strong reflections with highly non-stationary statistics. An antipersonnel mine(AP) can have a diameter as low as 2cm whereas many soils have very high attenuation frequencies above 3GHZ. The landmine detection problem can be solved by carrying out system level analysis of the issues involved to synthesise an image which people can readily understand. The *SIMCA* ('*SIM*ulated *C*orrelation *A*lgorithm') is a technique that carries out correlation between the actual GPR trace that is recorded at the field and the ideal trace which is obtained by carrying out GPR simulation. The *SIMCA* algorithm firstly calculates by forward modelling a synthetic point spread function of the GPR by using the design parameters of the radar and soil properties to carry out radar simulation. This allows the derivation of the correlation kernel. The SIMCA algorithm then filters these unwanted components or clutter from the signal to enhance landmine detection. The clutter removed GPR B scan is then correlated with the kernel using the Pearson correlation coefficient. This results in a image which emphasises the target features and allows the detection of the target by looking at the brightest spots. Raising of the image to an odd power >2 enhances the target/background separation. To validate the algorithm, the length of the target in some cases and the diameter of the target in other cases, along with the burial depth obtained by the *SIMCA* system are compared with the actual values used during the experiments for the burial depth and those of the dimensions of the actual target. Because, due to the security intelligence involved with landmine detection and most authors work in collaboration with the national government military programs, a database of landmine signatures is not existant and the authors are also not able to publish fully their algorithms. As a result, in this study we have compared some of the cleaned images from other studies with the images obtained by our method, and I am sure the reader would agree that our algorithm produces a much clearer interpretable image.**

I. Introduction

More than 110 million AP mines are estimated to be in the ground around the world.[1] Most AP mines are small, about 60 to 120mm diameter and 40 to 70mm thick and made of wood or plastic. The trigger mechanism in most AP mines has litte or no metal. The small size and the fact that many have little or no metal make them extremely difficult to detect using conventional technologies. The antenna reflections and the predominant soil surface can hide or change the response of the landmine. The *SIMCA* algorithm can however provide the operator with an image which is easy to interpret.

GPR signals contain not only the target response, but also unwanted effects from antenna coupling, system ringing and soil reflections that prevent the proper detection of the target. *SIMCA* removes various clutter such as cross talk, initial ground reflection and antenna ringing. We propose on reducing clutter by subtracting from each of the A scan an averaged value of an ensemble of A scan and also using windowed average subtraction method[Sengodan and Javadi [1]].

The collection of objects that might have generated the observed traces can be found by the correlation of the ideal point reflector traces and the actual traces obtained by the GPR.

Using *GprMAX2D v1.5* (a GPR simulator) developed by Giannopoulos [2]; the trace that would be generated by the ideal point relector can be generated. The simulator solves Maxwells equations using the finite-difference-time-domain model and this allowed the derivation of a mathematical model of the response of a point reflector.

By using Pearson's correlation coefficient between two variables which is defined as the covariance of the two variables divided by the product of their standard deviations we calculate the area correlation between the point reflector trace and the actual clutter removed GPR trace:

$$\rho_{X,Y} = \frac{E\left[(X - \mu_X)(Y - \mu_Y)\right]}{\sigma_X \sigma_Y} \tag{1}$$

This produced the correlated image where the brightest spots give the location of the target. In image processing, area correlation can give sub-pixel accuracy in locating the source of targets[Siebert et al[3] Chapter 6, section 6.6 pp. 2380]. Then raising the image to an odd power greater than 2 causes the target/background separation to be enhanced.

We then use a number of visualization techniques such as mesh generation and the correlated image with brightness raised to power of 3 to present the final images produced by the *SIMCA* algorithm. Figure 1 shows the flowchart of *SIMCA* algorithm.

The *SIMCA* algorithm has been used with success in locating foundations in demolished buildings [4].

[1] http://www.the-monitor.org/index.php

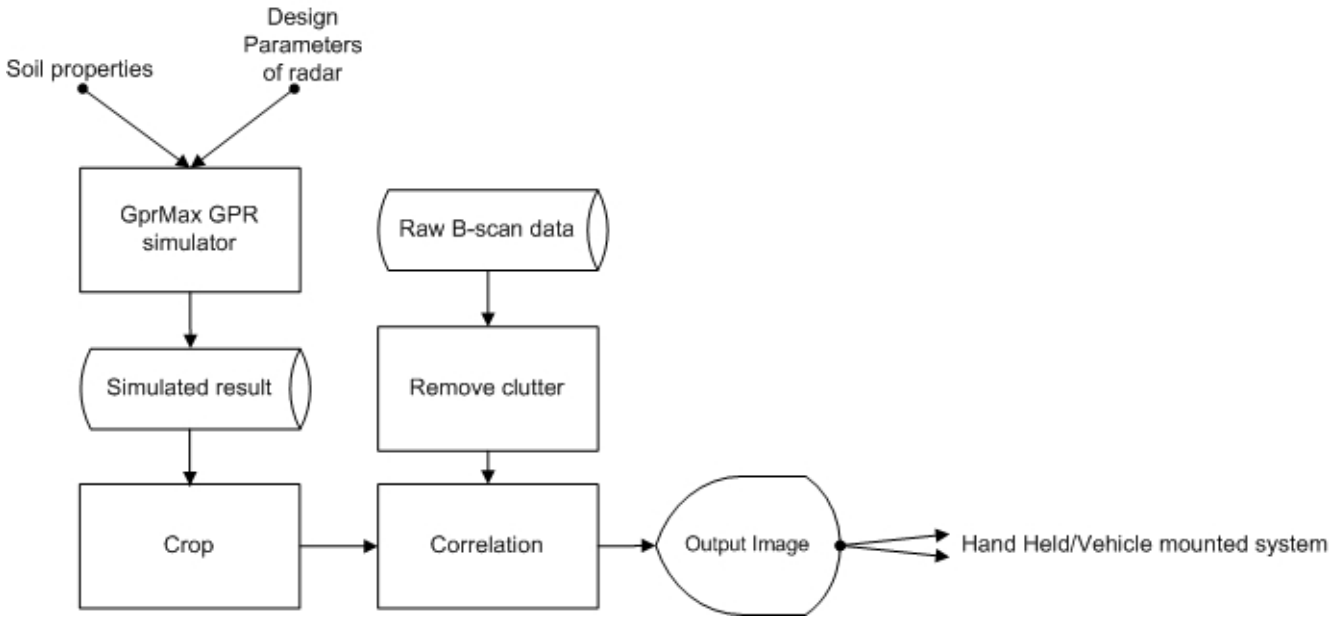

Fig. 1. The flowchart of the SIMCA *algorithm*

II. Prior Work

Migration is a technique that is used to move objects in a GPR image from where they appear to be, to where they actually are located in real life. The GPR data is misrepresented because of the structure of the transmitted pulse and also because of the signal spread of the GPR.

Stolt migration and in its general form, the phase shift migration [Gazdag[5]], uses the wave equation to backpropagate the recieved signal back to its source, and thereby obtains an image of the subsurface reflecting structures.

Song et al[6] integrate a fast nonuniform fast fourier transform (NUFFT) into the phase shift migration to reconstruct the target. Song et al state 'that a good reconstruction of the target is not obtained using phase-shift migration because its wavenumber space is not uniformly sampled as a result of the nonlinear relationship between the uniform frequency samples and the wavenumbers'.

Leuschen et al[7] use 'scattering theory along with a matched-filter response technique' for the GPR problem to develop a migration algorithm.

The novely of our proposed *SIMCA* algorithm lies in the fact that although wave theory is used by the above techniques, none of the algorithms report using different soil properties or radar properties for each unique test situation. Using the corresponding radar properties along with the soil conditions is an important factor in obtaining a good re-construction of the mine target.

To go further, none of the techniques available report on using correlation but rather use convolution. Correlation is better because it compensates for differences in gain and black level between the kernel and the area of the image being matched.

III. EXPERIMENTAL DATA SOURCE

The GPR data used for this experiment was obtained from Indian researchers at the Insitute of Technology. The GPR used for data acquisition is called the *SPRScan* commercial system and was developed by ERA Technology, UK. The system usually acquires a number of 195 A-scans, of 512 points each, with 16 bit resolution and a maximum equivalent sampling rate of 40 GHz.

Manufacturers recommendation is to use an operational time varying gain of 0.4 db/ns to partially compensate for the soil attentuation. So as to be able to store one A-scan each, the acquired data has to be buffered in two '*First in First out*' principles and is displayed in real time as a scrolling B-scan on the screen of a PC.

The pulse generator has a pulse width of 200ps and a repetition rate of 1MHz. The antenna's nominal bandwidth is 800 MHz to 2.5 GHz, hence leading to an expected resolution of less than 5cm.

A large sandbox which is aprroximately 9.9m x 7.8m was used and the scans were repeated for varying soil conditions. The stored mine file consisted of 24 stacked B-scans taken at 2.0cm intervals and each B-scan consisted of 102 A-scans. The A-scans are taken every 1.0cm and the effective sampling rate is 40 GHz.

Various mines developed by the Columbian guerrillas, various landmines and interfering objects such as tree roots and metal plate which can all cause serious false alarms where included to see how the algorithm performed. The GPR head was mounted on a platform and used a robotic head to acquire data.

IV. RESULTS

By using synthetic data we firstly validated the algorithm to ensure that it produced meaningful results.

We then proceeded to actual GPR data and used various visualization methods such as raising the brightness value to a higher power and the generation of a mesh of the correlated results using *MATLAB*.

Figure 2 shows the results of the two methods described above and the location of the plastic BAT/7 antitank mine can be clearly seen. The *SIMCA* method allows plastic mines to be detected and this is important because of the wide presence of plastic landmines. Also the mesh generated using *MATLAB* in Figure 2 shows the location of this plastic mine.

A. Results for the rest of the data and validation of the results

The use of the *Amira* software enabled the length of the target, diameter of the target and the burial depth to be determined. *Amira* is a visualization system and allows visualization of GPR data sets. By loading the 2D B scans and drawing a bounding box around the location of the target will allow the *Amira* system to give the length of the target in some cases and the diameter of the target in other cases along with the co-ordinates for the centroid of the object. From this centroid the burial depth of the target can be determined. It is to be noted that the correlated image with brightness raised to the power of 3 as shown in Figure 2B is loaded into the *Amira* system in order to obtain the above mentioned values.

The experiment was repeated for a large dataset and produced good results, but this paper sumarises the key results. Table I shows the actual lenghts of the targets and the actual burial depths of the targets along with the respective lengths and burial depths obtained using the *SIMCA* system. From Table I it can be seen that the *SIMCA* system can accurately give the length of the target and the maximum error rate is only 4.7%, whereas the minimum error rate is as low as 0.8%. This table also shows that for the burial depth, the *SIMCA* system is able to find out the burial depth with a maximum error rate of 4.4% and a minimum error rate of only 2.6%. The pleasing thing to note from this Table I is that for the plastic PFM-1 mine, which is a very small antipersonnel scatter mine the error rates are 2.5% and 4.3% for the error in the length and burial depth respectively. This PFM-1 mine is in essence a plastic bag containing explosive liquid and is a principal target ofr the International Campaign to Ban Landmines.

Table II shows the actual diameters of the targets and the actual burial depths along with their corresponding values estimated from the *SIMCA* system. Again, it can be noticed that the *SIMCA* system produces acceptable results.

Figures 3 and 4 give the error plot of the the estimated depths versus actual depth for both Table I and Table II. The charts also shows the linear trend lines for both graphs. From the graphs it is noticeable that the results are acceptable as indicated by the closeness of the predicted and actual depths.

V. COMPARISON WITH OTHER STUDIES

The authors compared the ***SIMCA*** algorithm with a number of current techniques, but for the purposes of this paper present two methods which were quite close to the SIMCA method. However the ***SIMCA*** algorithm outperforms its nearest rivals.

1) AL-NUAIMYA ET AL: Al-Nuaimya et al produce a developed system comprising a neural network classifier, a pattern recognition stage, and additional pre-processing, feature-extraction and image processing stages [8].

2) SAI AND LIGTHART: Sai and Ligthart improve the image by combining successive processing and spatial variable moving averaging to eliminate the clutter and to enhance the detection landmines [9] .

3) Overall Comparison: Figure 5[B] compares the methods with the SIMCA algorithm. Figures 5[A] and 5[C] shows images produced by the various techniques. ***SIMCA*** algorithm outperforms the above three methods.

VI. CONCLUSION

The proposed *SIMCA* algorithm is a practical tool in the detection of targets such as landmines. The authors have also used the algorithm to locate foundations in demolished building with success.

To validate the algorithm, the target length in some cases and the target diameter in other cases, along with the burial depth obtained by the *SIMCA* system are compared with the actual values used during the experiment in terms of the burial depth and the values based on the actual length or diameter of the real target.

The authors now plan on using 3D techniques using C scans because such 3D techniques enable the deminer to visualize the data volume to its entirety using a single image.

REFERENCES

[1] A. Sengodan and A. Javadi, "Landmine detection using masks on ground penetrating radar images", *IRIS 2005*.

[2] A. Giannopoulos, "GprMax software and manual, http://ww.gprmax.org/.

[3] P. J. Siebert, C. Boguslaw, "An introduction to 3D computer vision techniques and algorithms", *John Wiley and Sons Inc* Dec 2008.

[4] A. Sengodan, W. P. Cockshott and C. Cuenca-Garcia, "The SIMCA algorithm for processing Ground Penetrating Radar data and its use in locating foundations in demolished buildings", *2011 IEEE RadarCon conference,* pp. 706-709, May 2011.

[5] J. Gazdag, "Wave equation migration with the phase shift method", *Geophysics,* vol. 43, pp. 1342-1351, 1978.

[6] J. Song, Q. H. Liu, P. Torrione and L. Collins, "Two-dimensional and three-dimensional NUFFT migration method for landmine detection using Ground Penetrating Radar", *IEEE Trans. Geoscience. Remote Sensing,* vol. 44, No.6, pp. 1462-1469, June 2006.

[7] C. Leuschen and R. G. Plumb, "A matched-filter-based reverse-time migration algorithm for Ground-Penetrating Radar data", *IEEE Trans. Geoscience. Remote Sensing,* vol. 39, No.5, pp. 929-936, May 2001.

[8] W. Al-Nuaimy, Y. Huang, M. Nakhkash, M.T.C. Fang, V.T. Nguyen, and A. Eriksen, "Automatic detection of buried utilities and solid objects with GPR using neural networks and pattern recognition", *Journal of Applied Geophysics,* vol. 43, Issues 2-4, pp. 157-165, March 2000.

[9] B. Sai and L. P. Ligthart, "Effective clutter removal for detecting non-metallic mines in various soil fields", *IEEE Trans. on Geosc. and Remote Sensing*, 2003.

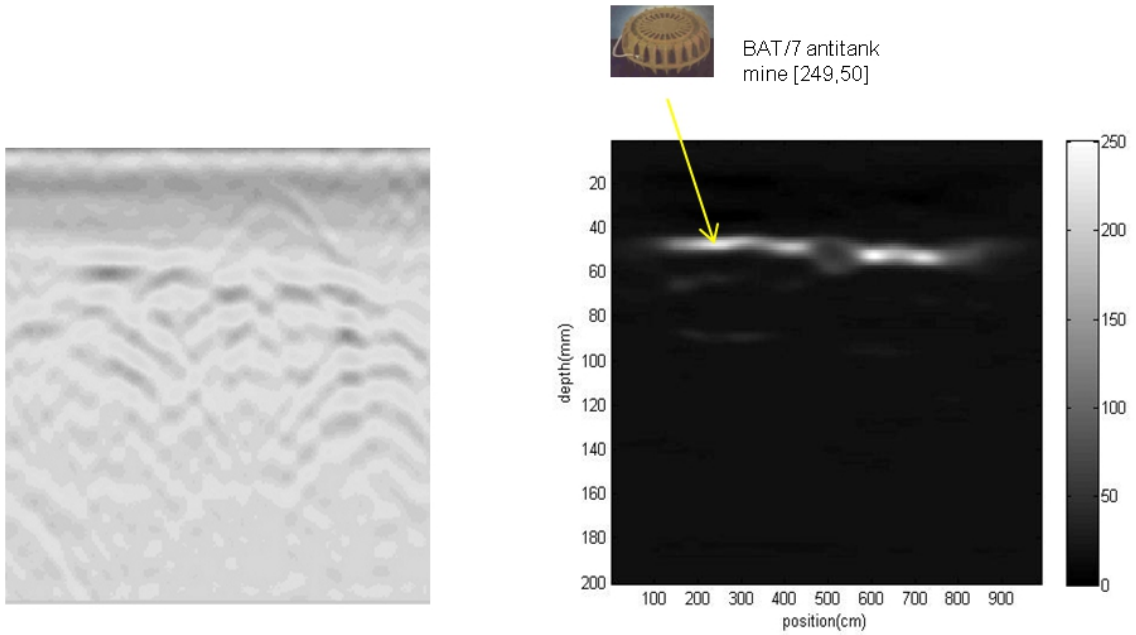

[A]

[B]

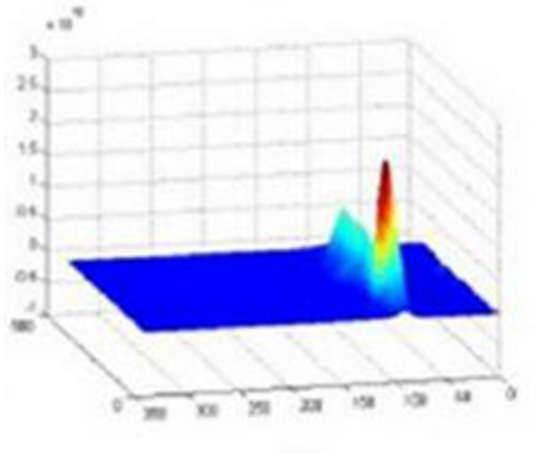

[C]

Fig. 2. From clockwise from left- [A]: Raw cleaned image; [B]: Correlated image with brightness raised to power of 3; The non-linear operation of raising to the power identifies the correct peak area; [C]: Mesh generated with MATLAB and the above figure has also been rotated in MATLAB to allow user to predict the location of the target from the visual depth.

TABLE I

ACTUAL LENGTH OF TARGET, ACTUAL BURIAL DEPTH, LENGTH OF TARGET OBTAINED FROM THE *SIMCA* METHOD, BURIAL DEPTH OBTAINED FROM THE *SIMCA* METHOD, PERCENTAGE ERROR FOR OBTAINING LENGTH OF TARGET USING *SIMCA* SYSTEM AND PERCENTAGE ERROR FOR OBTAINING BURIAL DEPTH USING *SIMCA* SYSTEM. BOTH THE LENGTHS AND BURIAL DEPTHS ARE IN MILLIMETRES.

	Ground truth		SIMCA			
	Length	Burial depth	Length	Burial depth	Error in length	Error in burial depth
Plastic APM-1	315	55	327	53	3.8%	3.6%
Plastic APM 29	265	49	253	51	4.5%	4.1%
Plastic AVM 195	620	68	615	70	0.8%	2.9%
Plastic FMK-3	244	71	240	74	1.6%	4.2%
Metallic Model 36	267	45	270	47	1.1%	4.4%
Wooden Model 43	190	56	181	54	4.7%	3.6%
Plastic No. 4	135	78	131	80	3.0%	2.6%
Plastic PFM-1	120	46	117	48	2.5%	4.3%
Wooden PMD-6	180	48	175	50	2.8%	4.2%

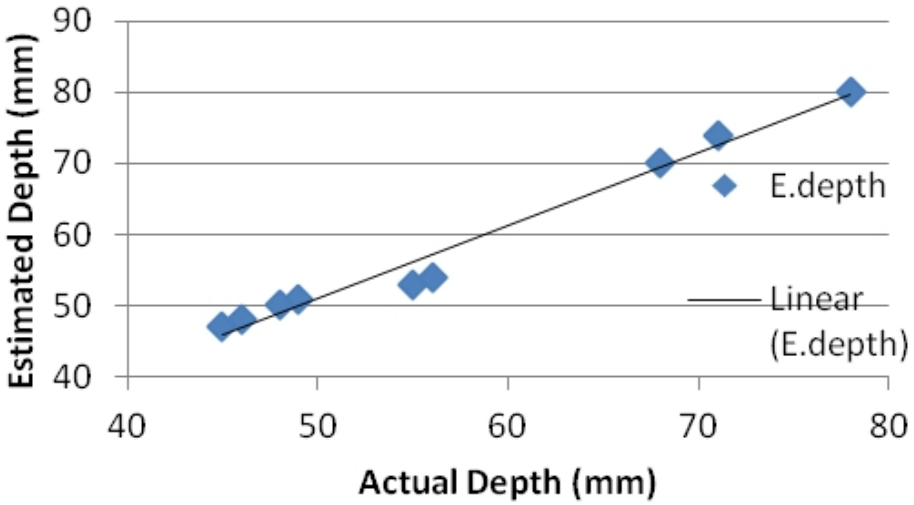

Fig. 3. Error Plots of Estimated depth versus the actual depth for Table I. The graphs also plot the linear trendline.

TABLE II

ACTUAL DIAMETER OF TARGET, ACTUAL BURIAL DEPTH, DIAMETER OF TARGET OBTAINED FROM THE *SIMCA* METHOD, BURIAL DEPTH OBTAINED FROM THE *SIMCA* METHOD, PERCENTAGE ERROR FOR OBTAINING DIAMETER OF TARGET USING *SIMCA* SYSTEM AND PERCENTAGE ERROR FOR OBTAINING BURIAL DEPTH USING *SIMCA* SYSTEM. BOTH THE DIAMETER AND BURIAL DEPTHS ARE IN MILLIMETRES.

	Ground truth		SIMCA			
	Diameter	Burial depth	Diameter	Burial depth	Error in length	Error in burial depth
Plastic VS-Mk2	90	53	87	55	3.3%	3.8%
Plastic AUS 15/50	125	52	127	53	1.6%	1.9%
Plastic BAT/7	270	89	259	86	4.1%	3.4%
Plastic M14	56	53	55	51	1.8%	3.8%
Metallic M26	79	52	77	54	2.5%	3.8%
Plastic MAUS	89	51	87	50	2.2%	2.0%
Cast Iron OZM-4	60	51	59	49	1.7%	3.9%
Plastic PRB M409	82	56	84	55	2.4%	1.8%
Plastic T/79	86	53	88	52	2.3%	1.9%

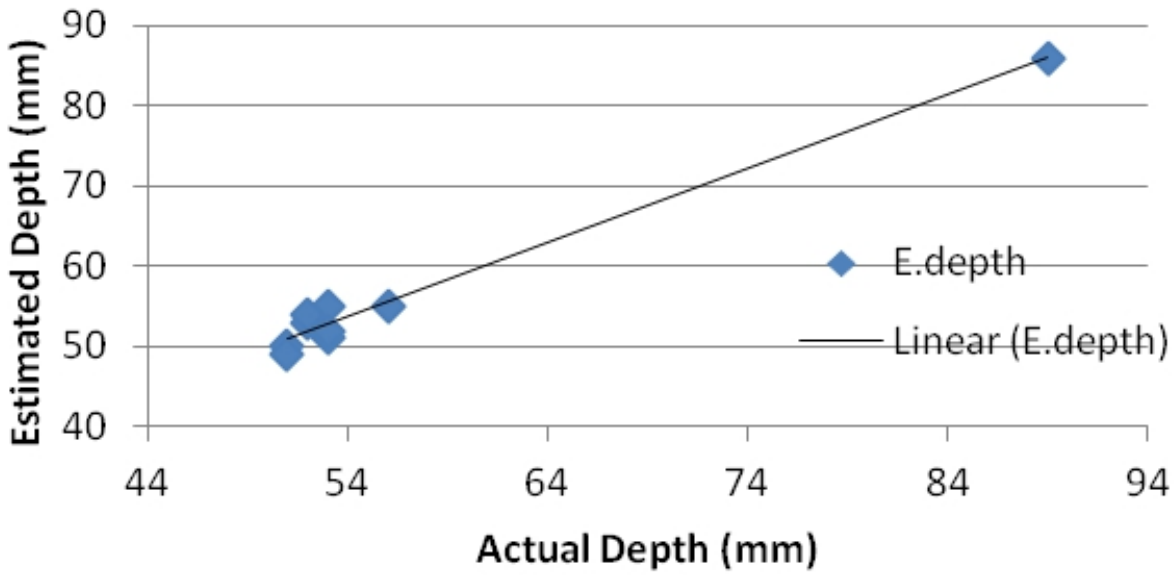

Fig. 4. Error Plots of Estimated depth versus the actual depth for Table II. The graphs also plot the linear trendline.

[A]

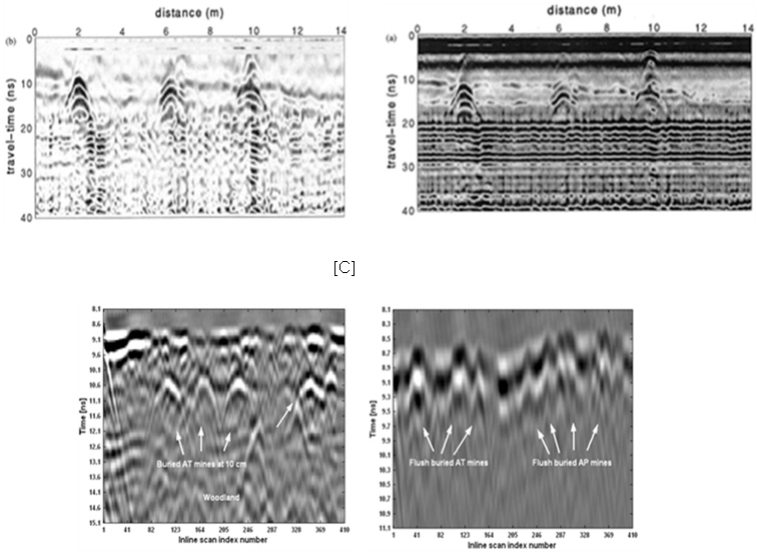

[C]

[B]

Sengodan and Cockshott	• **Location of target easy to interpret** • **No unwanted artifacts** • **No excessive depth echoing**
[A]: Al-Nuaimya et al	• No major difference between raw and cleaned image • The cleaned image has introduced more artifacts
[C]: Sai and Ligthart's	• Although image slightly cleaned some artifacts not removed • Not easy to isolate location of target

Fig. 5. From clockwise from left- [A]: Study by Al-Nuaimya et al who use a neural network classifier, a pattern recognition stage and additional pre-processing, feature extraction and image processing; [B]: Comparison of our study with the other two techniques; [C] Study by Sai and Ligthart who use a technique which combines successive processing and spatial variable moving averaging to eliminate the clutter.